

Demixing of Soft Particles

Bachelor's Thesis in Physics

presented by

Martin Majewski

January 27, 2020

Institute for Theoretical Physics I
Friedrich-Alexander-Universität Erlangen-Nürnberg



Supervisors:

Prof. Dr. Michael Schmiedeberg

Matthias Gimperlein, M.Sc

Abstract

In this work we try to reproduce demixing of invasive and non-invasive breast cancer cells, which occur in experiments. The system consists of two particle types which differ either by their potential, or by the strength of the activity of the particles. To investigate the properties of the system a simulation is established where the particle movement is governed by the Langevin equation. The external force is used to model a different stiffness of the particles by two types of pair wise interactions between the particles. Activity is modeled by oriented diffusion, variation in the diffusion step size are used to distinguish the particle types. In the case of different potentials and also in the case of different activity (with equal pair potentials), the system can be tuned such that the invasive particles diffuse to the surface of the ball, which is also recovered in experiments. The clustering of invasive cells and the formation of a hole in the ball could not be observed. But it is not excluded that with further fine tuning of the parameters this effects could happen.

Contents

1. Introduction	2
2. Theory	3
2.1. Spinodal Demixing	3
2.2. Langevin Equation	4
2.3. Pair Potentials	4
2.4. Active particles with orientational Diffusion	5
3. Simulation Model	6
3.1. Brownian Dynamic Simulations	6
3.2. Random Numbers	7
3.3. Initial Conditions	8
4. Data Analysis	9
4.1. Surface Ordering	9
4.2. Ordering Of The Particles	9
4.3. Direction Of Active Self-Propulsion	10
5. Results	10
5.1. Demixing By Size	10
5.2. Demixing By Stiffness	14
5.3. Demixing With Active Particles	18
6. Summary and Outlook	23
References	24
7. Eidesstattliche Erklärung	25

1. INTRODUCTION

In order to find a treatment for a disease one needs to understand how this disease behaves inside a human body. One of the diseases which is not understood yet is cancer. To fix this problem lots of experimentalists are currently working in this field [1] [2]. One main issue is the characterization of the tumor. The state of the art is to do a biopsy [3]. There are investigations how to improve this technique [4]. One of the main problems that is remaining is the question where to probe the tumor. Exact analytical models are, due to the large amount of unknowns, not possible. Therefore one can try to find model systems which can hint the main properties which lead to the creation of certain effects. In this work we tried to answer if the demixing of invasive and non-invasive breast cancer cells, which can be seen in experimental results [compare Figure 1], can occur due to a different stiffness of the cells or if it is necessary that the cells can actively move.

online not available



FIG. 1: Sectional image of a ball of tumor cells after an evolution of 24 hours. The cells were placed randomly inside an artificial tissue. Two types of cancer cells are mixed: Colored in magenta are the invasive (mesenchymal) cells. Colored in green are all cells (invasive and non-invasive). Observed is a demixing of the cells. The invasive cells tend to diffuse to the surface of the cell ball. Also a clustering of the invasive cells can be seen. Finally, in the upper right corner a region exists, which is free of any type of cells (group of Prof. Dr. Ben Fabry).

In section 2 the Langevin equation, which is the basis of many equilibrium and non-equilibrium many body simulations is established. In section 3 the details of the simulation are explained. In section 4 it is described how the simulation data is analyzed. Afterwards it is shown in section 5 which effect could possibly lead to the experimentally observed behavior. Finally a summary and a short outlook is given in section 6.

2. THEORY

2.1. Spinodal Demixing

The theory of demixing of particles in equilibrium is well understood [5]. When two types of particles are mixed in thermal equilibrium various things can happen. Depending on the particle ratio and on the temperature of the system the particles can form the so called homogeneous phase, where the particles are randomly mixed. They can form clusters in the 2-phase area or the system can be in the metastable area where a mixture of both phases can occur. This configuration is shown in Figure 2. But this theory does not apply in the case of cancer cells because of various reasons: First, such kind of a system is most likely not in equilibrium. Additionally we have local demixing and finally we are interested in the process of demixing. Therefore, one has to consider the very basic physics of this problem. So, we will start with Newton's equation.

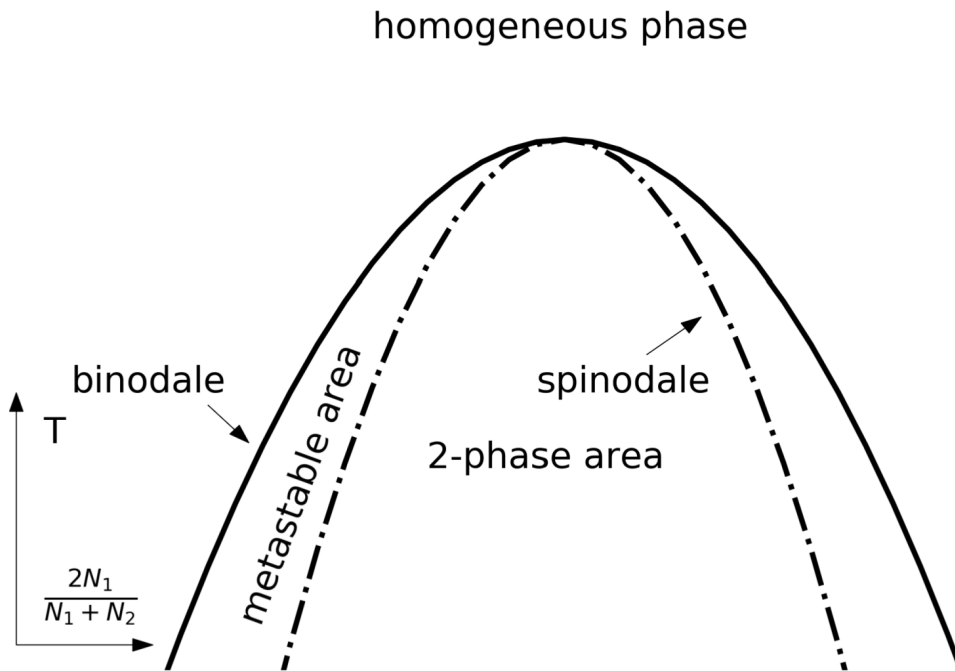


FIG. 2: Phase diagram of demixing phases for two different particle types. Shown is the separation into the homogeneous phase, where the particles are randomly mixed, the 2-phase area, where clusters of particles are forming and the metastable area where both can happen.

2.2. Langevin Equation

This section is based on [6] and [7].

We consider a classical system with N particles, for each particle i Newton's equation applies:

$$m_i \frac{d\vec{v}_i}{dt} = \vec{F}_i$$

Where m_i is the mass of the particle and \vec{v}_i is its velocity. The force \vec{F}_i on each particle can be split into two main components. The frictional force of the surrounding $\vec{F}_{fr}(t) = -\gamma\dot{\vec{x}}(t)$, is approximated by Stokes Law for hard balls. Therefore $\gamma = 6\pi\eta r$ holds. The second force is a rapidly fluctuating force $\vec{F}_T(t)$ due to the thermal impacts of the tissue. We assume that $\vec{F}_T(t)$ is

- independent of x
- varies extremely rapidly compared to the variation of $x(t)$ of a particle
- that the mean is $\langle \vec{F}(t) \rangle = 0$
- and that the second moment is $\langle \vec{F}_T^2 \rangle = \frac{6\gamma k_B T}{\Delta t}$

With these assumptions one can calculate the mean square displacement to be:

$$\langle \Delta x^2 \rangle = \frac{6k_B T}{\gamma} t \quad (1)$$

With an additional external force, which will model the pair wise interaction between the particles and the activity of the particles, we end up with the Langevin equation:

$$m \frac{d\vec{v}}{dt} = \vec{F}_{fr}(t) + \vec{F}_{ext} + \vec{F}_T$$

For the considered system the time $\frac{m}{\gamma}$ is very short compared to the interesting timescales. Therefore we can neglect inertia and ballistic regime:

$$\gamma \vec{v} = \vec{F}_{ext} + \vec{F}_T$$

This is the so-called overdamped Langevin equation.

2.3. Pair Potentials

The external force consists of two parts. The part which is always present is the pair potential between the particles. The potential models the interaction between the particles. To model the demixing of the invasive and non-invasive cells due to different stiffness, two different particle potentials are used. The potentials consists of an attractive and a repulsive part. The attractive part leads to an effective surface tension and the forming of a ball of particles. It is equal for both particle types. The range of the

interaction is set to be as long as the repulsive part of the potential starting at the end of the repulsive part. The repulsive part splits into two equally long parts, a harder core, where the particles can overlap only for a few time-steps and a weaker shoulder. The height of the shoulder can be varied for the different particle types. For simplicity the potentials consists only of straight lines. The interaction between the particle types is modeled by the average of the two potentials. An example set of potentials is shown in Figure 3.

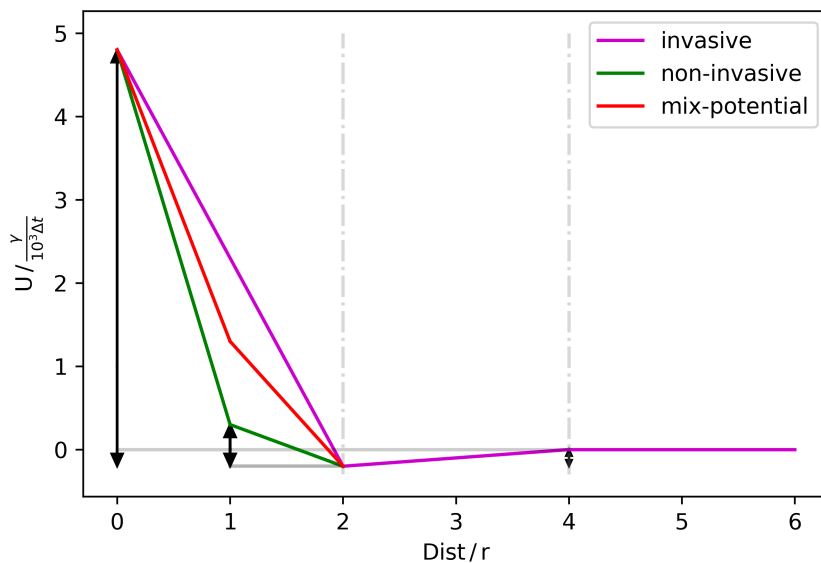


FIG. 3: Plot of the different potentials in dependence of the distance between the centers, where r is the particle radius. In purple the potential of invasive particles, in green of non-invasive particles and in red the potential for the interactions between the different particle types is shown. The black arrows indicate the parameters that can be varied.

2.4. Active particles with orientational Diffusion

There is a great variety for models of active particles. One of the simplest ones considers contact forces of self-repulsion along with orientational diffusion. It works as follows: Each particle additionally gets a normalized direction vector. In this case the direction of the vector is initially randomly chosen for all particles. In each time step a randomly chosen vector with the maximal length of a_c , which is perpendicular to the direction vector is added. Therefore the direction vector changes with time. Afterwards the particle makes, in addition to the Brownian motion and to the motion induced by the pair potential, a step of the size a_s in that direction and the direction vector is normalized again. A sketch of one step for an active particle due to oriented diffusion is shown in Figure 4.

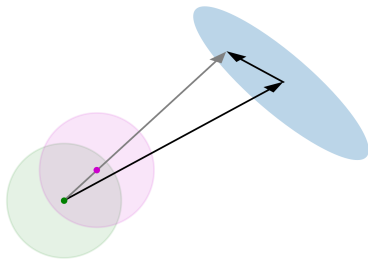


FIG. 4: Illustration of one iteration step of oriented diffusion. The original position of the particle is shown in green. The original activity direction vector is shown in black. The direction is changed by the small black arrow. The resulting direction is represented by the gray arrow. The blue area, which is perpendicular to the direction vector, indicates the possible changes of the direction, from which the change is randomly chosen. The particle is moved to the position shown in purple. The step size and the size of the change are exaggerated by at least a factor of 100.

3. SIMULATION MODEL

We model a system with N_1 particles of type 1 and N_2 particles of type 2 (usually 140 non-invasive and 40 invasive particles). As a typical length-scale we use $\frac{1}{2}$ of the length of the repulsive part of the particle potential, which will be called particle radius p_r . As simulation box we use a cube with a edge-length of $30 p_r$ and periodic boundary conditions.

3.1. Brownian Dynamic Simulations

The overdamped Langevin equation from section 2.2 is:

$$\gamma \vec{v} = \vec{F}_{ext} + \vec{F}_T$$

We can discretize the overdamped Langevin equation:

$$\vec{r}(t + \Delta t) = \vec{r}(t) + \frac{\Delta t}{\gamma} \left(\vec{F}_{ext}(t) + \vec{F}_T(t) \right)$$

This is the equation that is used to develop the system in the simulation. As a typical timescale we use the Brownian time which is defined as follows: $\Delta\tau = \frac{r^2}{D}$ where r is the radius of a particle and D the diffusion constant. After one Brownian time the mean square displacement of a particle due to diffusion is given by the square of the length of its radius. A step size of $\Delta t = 10^{-5} \Delta\tau$ is used.

3.2. Random Numbers

In this work random numbers are used to generate the initial conditions for the positions of the particles as well as for the initial direction of the activity (if present). They are also used during the simulation to generate random steps for the Brownian motion and for the change of the direction of the activity.

The random numbers in a sphere for the Brownian motion are calculated with three uniformly distributed random variables (ϕ , u and r). These are taken from the intervals $\phi \in [0, 2\pi]$, $\theta = \arccos(u)$ with $u \in [-1, 1]$ and $r \in [0, r_b]$. The Cartesian coordinates are then calculated via:

$$\begin{aligned}x &= r\sin(\theta)\cos(\phi) \\y &= r\sin(\theta)\sin(\phi) \\z &= r\cos(\theta)\end{aligned}$$

r_b is chosen such that it matches the mean square displacement of the Brownian motion. To see that for these choice of random numbers each direction is equally likely we consider the Inversion method [6] [8]. For the surface element of a sphere

$$dA = \sin(\theta)d\theta d\phi =: 4\pi f(\phi, \theta)d\theta d\phi$$

we have:

$$\begin{aligned}f(\phi) &= \int_0^\pi f(\phi, \theta)d\theta = \frac{1}{2\pi} \\f(\theta) &= \int_0^{2\pi} f(\phi, \theta)d\phi = \frac{\sin(\theta)}{2}\end{aligned}$$

We can use uniformly distributed random numbers for ϕ but for θ we need to consider something else. We take the cumulative distribution function of θ :

$$F(\theta) = \int_0^\theta f(\hat{\theta})d\hat{\theta} = \frac{1}{2}(1 - \cos(\theta))$$

The inverse function is:

$$F^{-1}(u) = \arccos(1 - 2u)$$

with $u \in [0, 1]$ uniformly distributed. Or equally:

$$F^{-1}(u) = \arccos(u)$$

with $u \in [-1, 1]$.

For the change of the direction of the activity one needs random numbers uniformly distributed on a circle with radius a_c . This is done by taking two random numbers r, ϕ , uniformly distributed in the interval $[0, a_c]$ and $[0, 2\pi]$. The Cartesian coordinates are then calculated via: $x = r\cos(\phi)$ and $y = r\sin(\phi)$.

3.3. Initial Conditions

The initial conditions turned out to be important for obtaining proper results. When the particles are placed randomly in the whole box, one will often not even observe the formation of a ball. Therefore different initial conditions were used in the simulation. The two more heavily used ones are described in more detail below.

Random initial condition



FIG. 5: Plot of the simulation box. Left: The smaller box indicates the region where the particles can be placed initially. Right: One possible realization of an initial setup with this configuration.

The particles are randomly placed inside a certain cubic volume inside the box. It is prevented that the particles are initially closer than p_r from center to center. The different particle types are placed one by one as long as only one particle type to set is left. Then the rest is placed. This results in slightly biased initial conditions. The particles with higher particle number are initially, on average, closer to the boundaries of the box. To be able to compare the simulations to the experimental data, the number of invasive particles in the simulations is smaller as the number of non-invasive particles. One of the effects we try to reproduce is that the invasive particles diffuse on average closer to the surface. Therefore it is bearable that they are initially closer to the center. One example configuration of this type is shown in Figure 5.

Biased initial condition

In the second configuration used as initial conditions the particles are also placed randomly, one type after the other, and with the restriction that they do not overlap initially. The particles are now placed in a certain distance interval to the center of the box. This interval can be tuned differently for the two particle types, eg. particle type one is placed in a distance from $0 p_r$ to $3 p_r$ and particle type two from $3 p_r$ to $8 p_r$. This initial condition is illustrated in Figure 6. This initial condition is used to simulate the

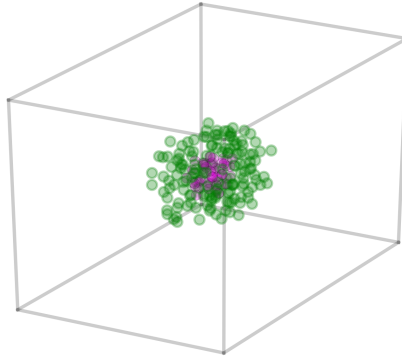


FIG. 6: Plot of the simulation box. The particles are placed as described in the example of section 3.3.

extreme cases, when one particle type is on the surface of the ball, while the other is inside.

4. DATA ANALYSIS

The goal of the simulation is to find a set of parameters which reproduces at least qualitatively the experimental data shown in Figure 1. In order to do so the effects are separated into different categories.

4.1. Surface Ordering

To get an overall impression if one particle type is more likely to be on the surface of the ball, the average distance to the center of mass for each particle type is calculated. The particles are assumed to have equal masses. The average distance to the center is called s_o .

4.2. Ordering Of The Particles

For a more detailed insight into the structure of the ball a histogram of the distances can be calculated for each particle type. For better statistics the data is averaged over multiple time-steps during the simulation. The number of time-steps are chosen such that the system has already reached a, at least, meta-stable state. The histogram is

normalized with respect to the particle number and then re-scaled with respect to $\frac{1}{r^2}$. This is due to the fact that the area of a certain distance of a point grows with r^2 .

4.3. Direction Of Active Self-Propulsion

It is tested if the directions of the activity of the particles align in some way. In order to do so the scalar product of position vector of each particle with respect to the center of mass and the activity direction vector, averaged over different distance intervals is calculated.

5. RESULTS

In this section the results are summarized. The results are split into demixing processes due to demixing by a different effective size of the particles, due to different stiffness and due to different activity. All of the systems seem to have many metastable states. Therefore, the outcome of a single simulation cannot be predicted. A full statistical analysis cannot be done due to the small number of simulations that can be made with reasonable computational effort. But usually already after a few simulations a tendency can be seen in the data.

5.1. Demixing By Size

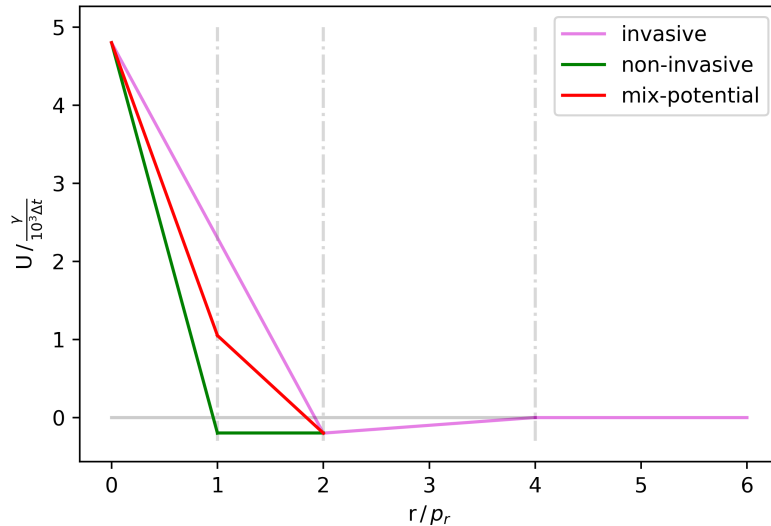


FIG. 7: The pair potentials of the particles types used in this sub-chapter. The potential of the invasive particles is shown in purple. The potential of the non-invasive in green. The potential for interactions between the particle types is shown in red.

The form of the potentials of the two particle types is shown in Figure 7. The potentials are tuned such that the non-invasive particles have no repulsion in the repulsive shoulder. Therefore, they have a next neighbor distance of approximately p_r from center to center in the final state. The invasive potential is tuned such that the core and the repulsive shoulder are equal in strength. This results in a next neighbor distance of approximately $2p_r$ for the invasive particles. Therefore, the particles have a different effective size. The interaction potential between the particle types is the average of the two potentials. There is no activity of the particles.

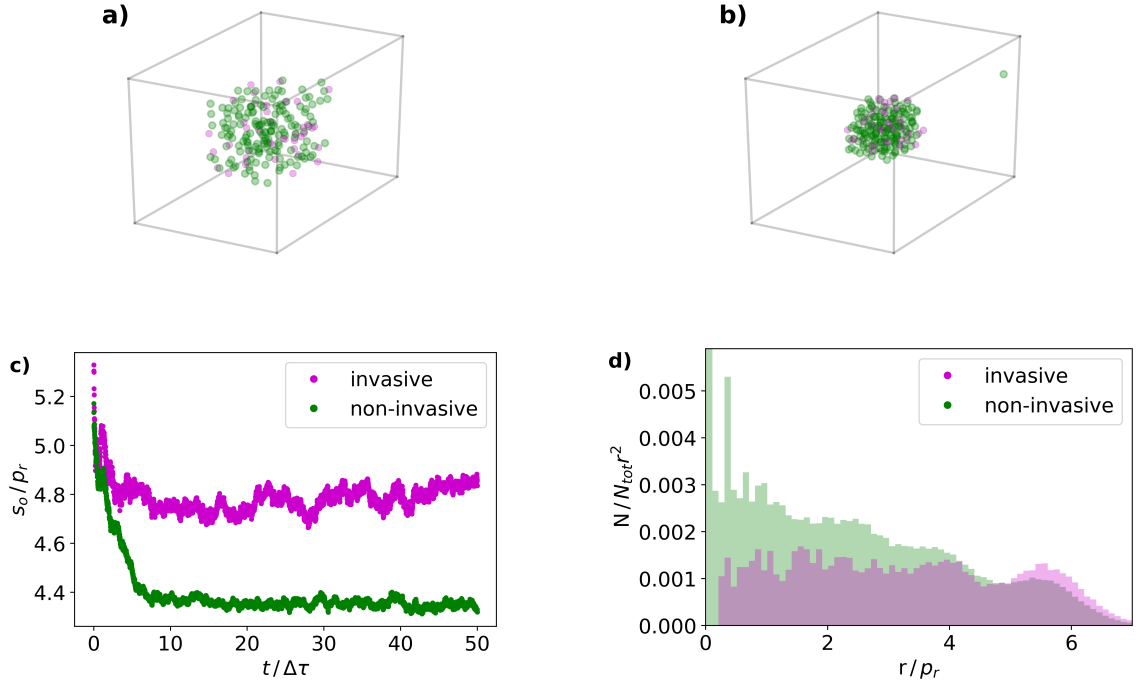


FIG. 8: Random initial conditions. The cells differ by the length of the repulsive potential. 10 simulations are averaged. **a:** One representative initial state. **b:** One representative final state. **c:** The development of the system averaged over the simulations. **d:** A histogram of the distances of the particle types to the center of mass, normed on the particle number N_{tot} , scaled with $\frac{1}{r^2}$, averaged over simulations and time.

In Figure 8 the particles are placed randomly. Observed is a large demixing of the particles occurring already while the ball is still forming. Nevertheless the invasive particles are not only on the surface of the cell ball. The probability to be in the center seems to be only slightly suppressed.

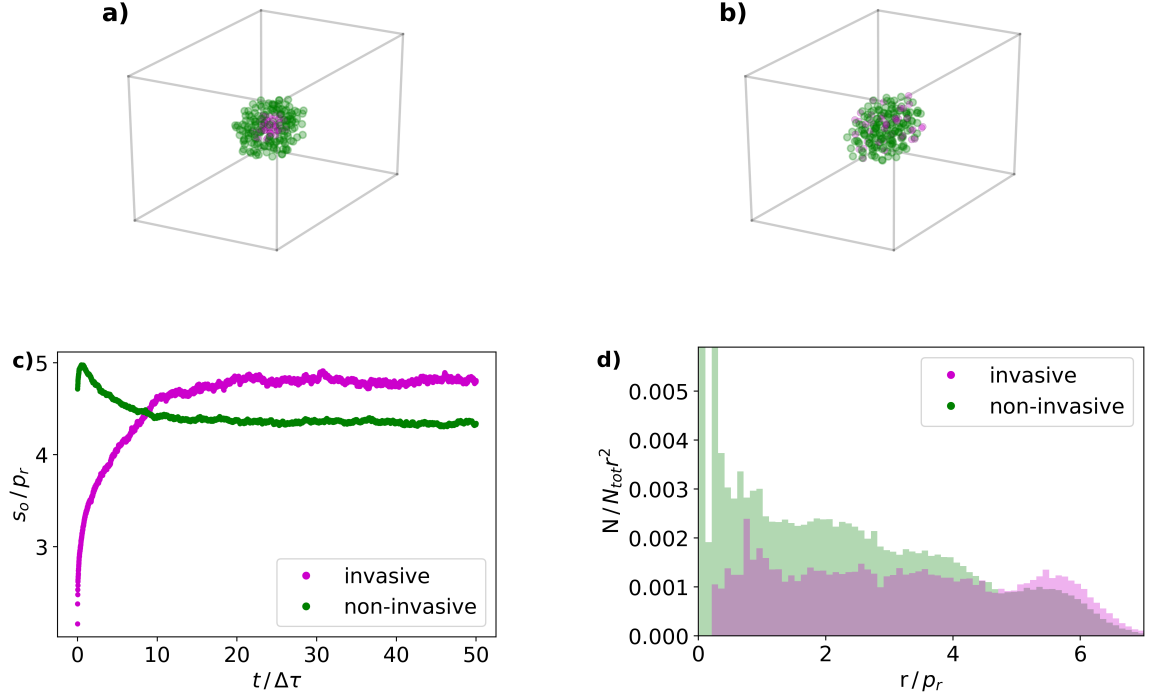


FIG. 9: Biased initial conditions. The invasive cells are set in a distance from $0 p_r$ to $4 p_r$ to the center, the non-invasive cells from $4 p_r$ to $6 p_r$. 10 simulations are averaged. **a:** Example of one representative initial state. **b:** One representative final state. **c:** The development of the system averaged over the simulations. **d:** A histogram of the distances of the particle types to the center of mass, normed on the particle number N_{tot} , scaled with $\frac{1}{r^2}$, averaged over simulations and time.

In Figure 9 the particles are placed in a biased way. The invasive cells are placed in the center of the ball. The non-invasive closer to the surface of the ball. The invasive particles diffuse relatively fast to the surface, but not all invasive particles are finally on the surface. Some find a metastable place on any distance to the center of the ball. The behavior of the system after about $20 \Delta\tau$ seems to be quite similar as with random initial conditions.

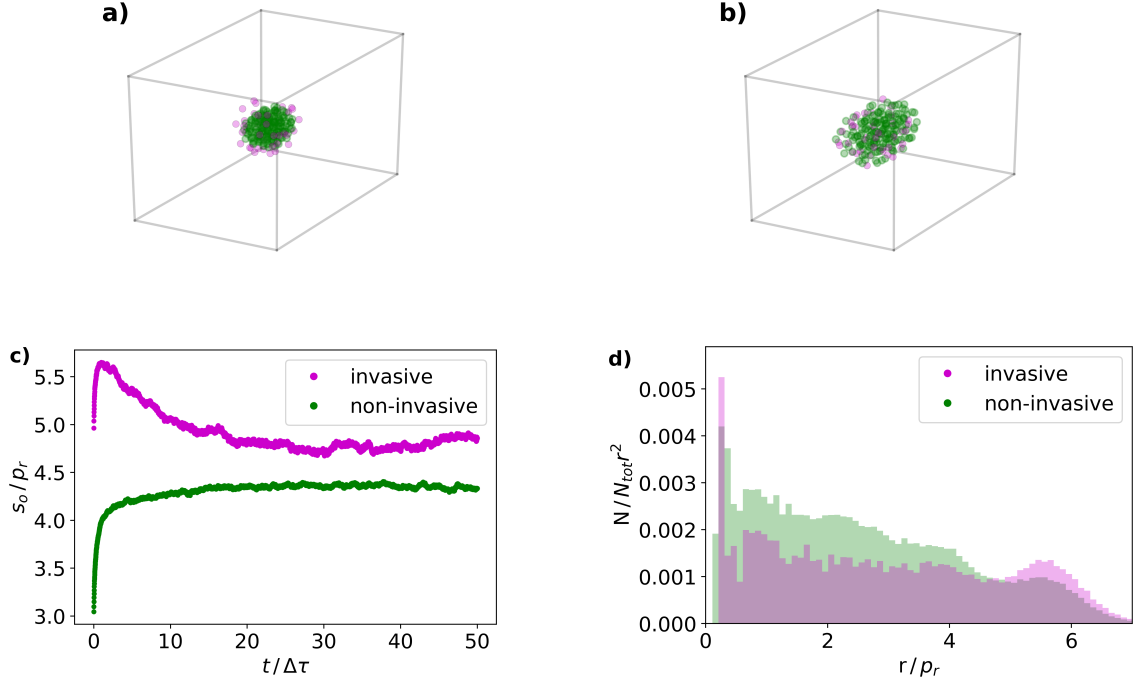


FIG. 10: Biased initial conditions. The invasive cells are set in a distance from $4 p_r$ to $6 p_r$ to the center, the non-invasive cells from $0 p_r$ to $4 p_r$. 10 simulations are averaged. **a:** Example of one representative initial state. **b:** One representative final state. **c:** The development of the system averaged over the simulations. **d:** A histogram of the distances of the particle types to the center of mass, normed on the particle number N_{tot} , scaled with $\frac{1}{r^2}$, averaged over simulations and time.

In Figure 10 the particles are placed in a biased way. The non-invasive particles are set in the center of the ball, the invasive ones closer to the surface. Surprisingly some of the invasive cells do not stuck to the surface, but diffuse inside. But most of the invasive particles stay on the surface. Therefore we get a long time behavior which is quite similar to the other two initial conditions.

With different effective sizes of the particles one observes the diffusion of the invasive particles to the surface. The long time behavior of the system seems to be quite stable to changes in the initial condition. What is not observed, compared to the experimental data in Figure 1, is a clustering of the invasive cells inside the ball. Also missing is a hole in upper half of the tumor, which is present in the experiment. It seems to be unlikely that a different radius is the driving force in this process, because this could have been easily confirmed in experiments by measuring the size of the particles.

5.2. Demixing By Stiffness

The form of the potentials used in this sub-chapter is shown in Figure 11. It is very similar to the previous one. The difference is that the slope of the attractive part of the potential is doubled compared to the previous simulations. This increased surface tension is compensated via an increased repulsive potential in the region next to the center. The relatively big ratio between the slopes of the repulsive parts of the potentials is needed to prevent a collapse of the system to a point. The particle types mainly differ in the slope of the potential in the region from p_r to $2p_r$ indicating different stiffness of the shoulders. The slope of the potential of the invasive particles is double of the slope of the non-invasive ones. The interaction between the particles is as usual the mean of both potentials. The repulsive force of the shoulder is not strong enough to overcome the attractive regime. Hence most of the particles (independently of the type) have a next-neighbor distance of approximately p_r . There is again no activity of the particles.

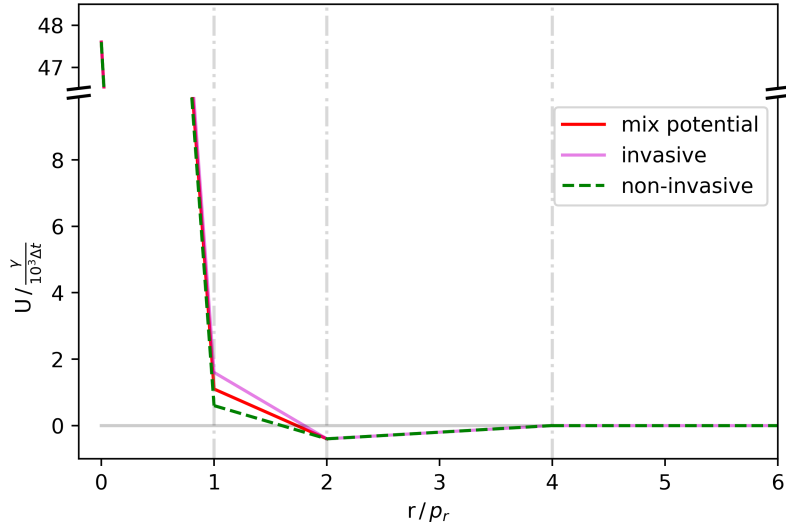


FIG. 11: The pair potentials of the particles types used in this sub-chapter. The potential of the invasive particles is shown in purple. The potential of the non-invasive in green. The potential for interactions between the particle types is shown in red. The huge stiffness of the core is needed to compensate a slightly higher surface tension.

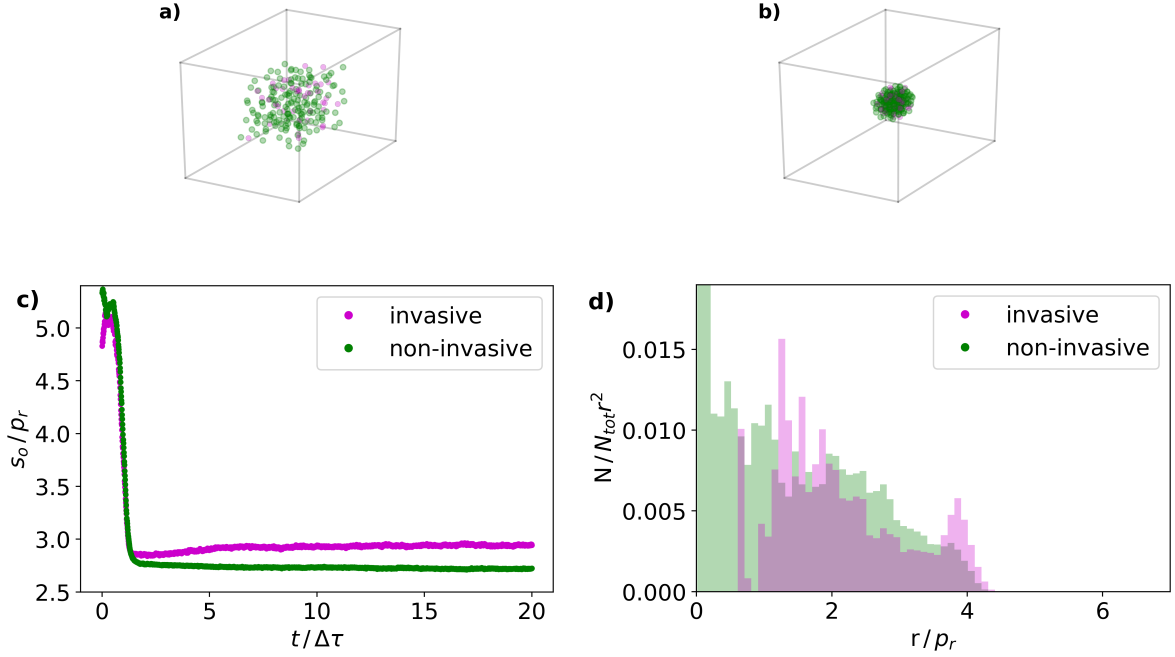


FIG. 12: Random initial conditions. The cells differ only by the strength of their repulsive potential. 6 simulations are averaged. **a:** Example of one representative initial state. **b:** One representative final state. **c:** The development of the system averaged over the simulations. The invasive cells have a slightly higher probability to be on the surface of the ball due to their harder core. **d:** A histogram of the distances of the particle types to the center of mass, normed on the particle number, scaled with $\frac{1}{r^2}$, averaged over simulations and time. The main difference in the occupation of the different particle types seems to be in the center of the ball and on the surface.

In Figure 12 the particles are placed randomly. Observed is a formation of a ball which is smaller than in Figure 8. Afterward an very slow and slightly demixing occurs. Also the probability of the particles to be in a certain distance to the center is quite different to the case with different sizes of the particles. Now it seems to be very unlikely for the invasive particles to be near the center of the ball, while in the case of different sizes the probability was equally distributed over the distance to the center. Similarly on the surface of the ball there is a higher probability to find an invasive particle although the bias seems to be a bit higher compared to the demixing due to different size.

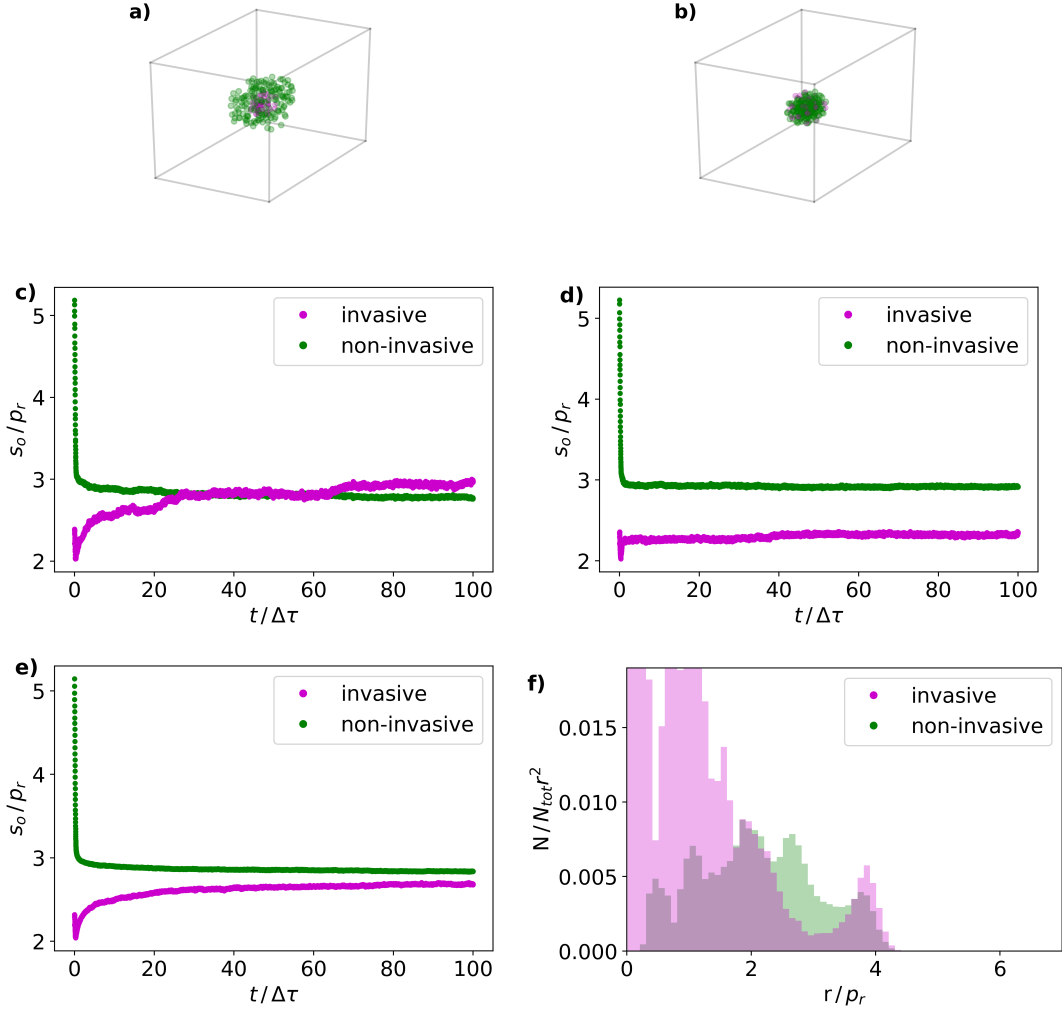


FIG. 13: Biased initial conditions. The invasive cells are set in a range from $0 p_r$ to $3 p_r$ to the center, the non-invasive ones form $3 p_r$ to $7 p_r$. 10 simulations are averaged. The cells differ only by the strength of the repulsive potential. **a:** Example of one representative initial condition. **b:** One representative final state. **c:** Extreme case, where the reorganization of the particles is largest. **d:** Extreme case, where the cells fall into a metastable state which is very similar to the initial condition. **e:** The development of the system averaged over all 10 simulations. The invasive cells seem to diffuse slowly to the surface of the ball. **f:** A histogram of the distances of the particle types to the center of mass, normed on the particle number, scaled with $\frac{1}{r^2}$, averaged over simulations and time.

In Figure 13 the particles are placed in a biased way. The invasive cells are set inside the ball, while the non-invasive particles are set on the surface. Observed is a reorganization of the particles. Some invasive particles diffuse to the surface of the ball and stuck there, while the main part is forming a cluster at the center of the ball. This reorganization takes place on a much longer timescale than in the case of particles with

different sizes [Figure 9]. In Figure 13f interesting observations can be made. While the main part of the invasive particles are still stuck inside the ball, there is already a higher density of invasive particles on the surface of the ball.

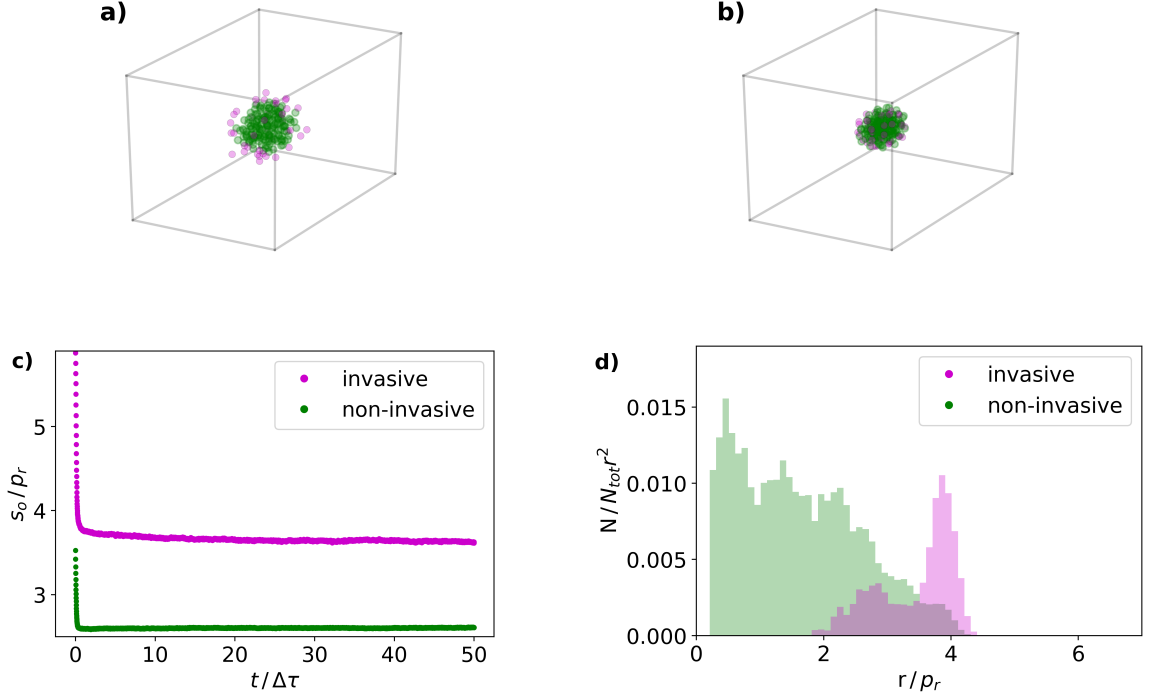


FIG. 14: Biased initial conditions. The non-invasive cells are set in a range from $0 p_r$ to $5 p_r$ to the center, the invasive ones from $5 p_r$ to $7 p_r$. 10 simulations are averaged. The cells differ only by the strength of the repulsive potential. **a:** Example of one representative initial condition. **b:** One representative final state. **c:** The development of the system averaged over all 10 simulations. In the beginning there is a relaxation to a dense ball of cells, after that no changes are observed. **d:** A histogram of the distances of the particle types to the center of mass, normed on the particle number, scaled with $\frac{1}{r^2}$, averaged over simulations and time.

In Figure 14 the particles are placed in a biased way. This time the non-invasive particles are set inside the ball, while the invasive ones are placed on the surface. We find that the starting configuration remains for a long time. The invasive particles penetrate only a bit into the ball, which is quite different compared to the case with different sizes of the particles. The center of the ball stays completely free of invasive particles.

The stiffness of the particle types seems to be one possible reason for a diffusion of the invasive particles to the surface. This time the development of the system is dependent on the initial condition. Again no clustering or building of holes is observed.

5.3. Demixing With Active Particles

Now we use active particles. Therefore the potentials, in this sub-chapter, for the two particle types are identical. The potential is sketched in Figure 15. The particles have an activity as described in section 2.4. The activity of the invasive particles is set to be 10 times larger than that of the non-active particles.

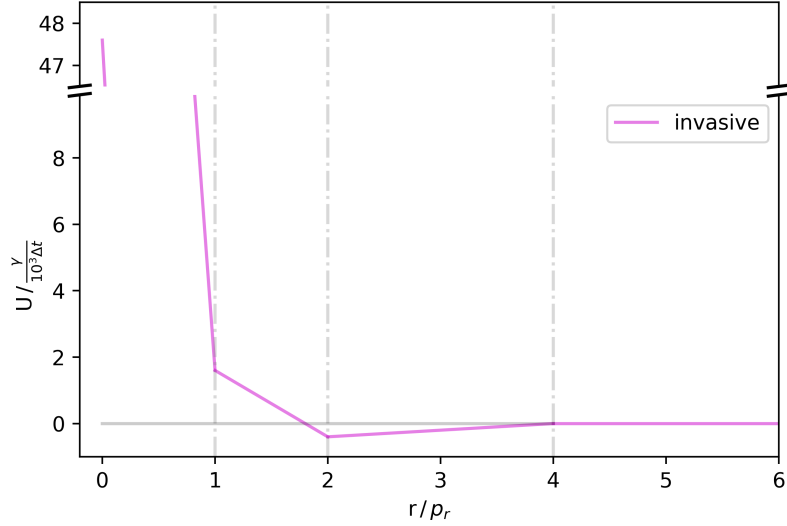


FIG. 15: The pair potential between the particles. In this sub-chapter the potential is equal for invasive and non-invasive particles. They differ only by the strength of their activity.

In Figure 16 the particles are set random. We find particles that are not captured in the ball. This also occurs for non-invasive particles, but it is far more likely for the invasive ones, due to the larger activity. The invasive particles also have a tendency to be nearer to the surface of the ball. It also seems that the invasive cells have some preferred and also some unsuitable distances to the center of the ball. In contrast to the case with the different stiffness of the particles the invasive cells can be also in the center of the ball.

The directions of the particle activities align themselves. In the center of the ball the directions seem to be random (larger fluctuations due to smaller particle numbers). With increasing distance to the center the directions of the invasive particles align more and more towards the surface. This effect is not observed for the non-invasive particles.

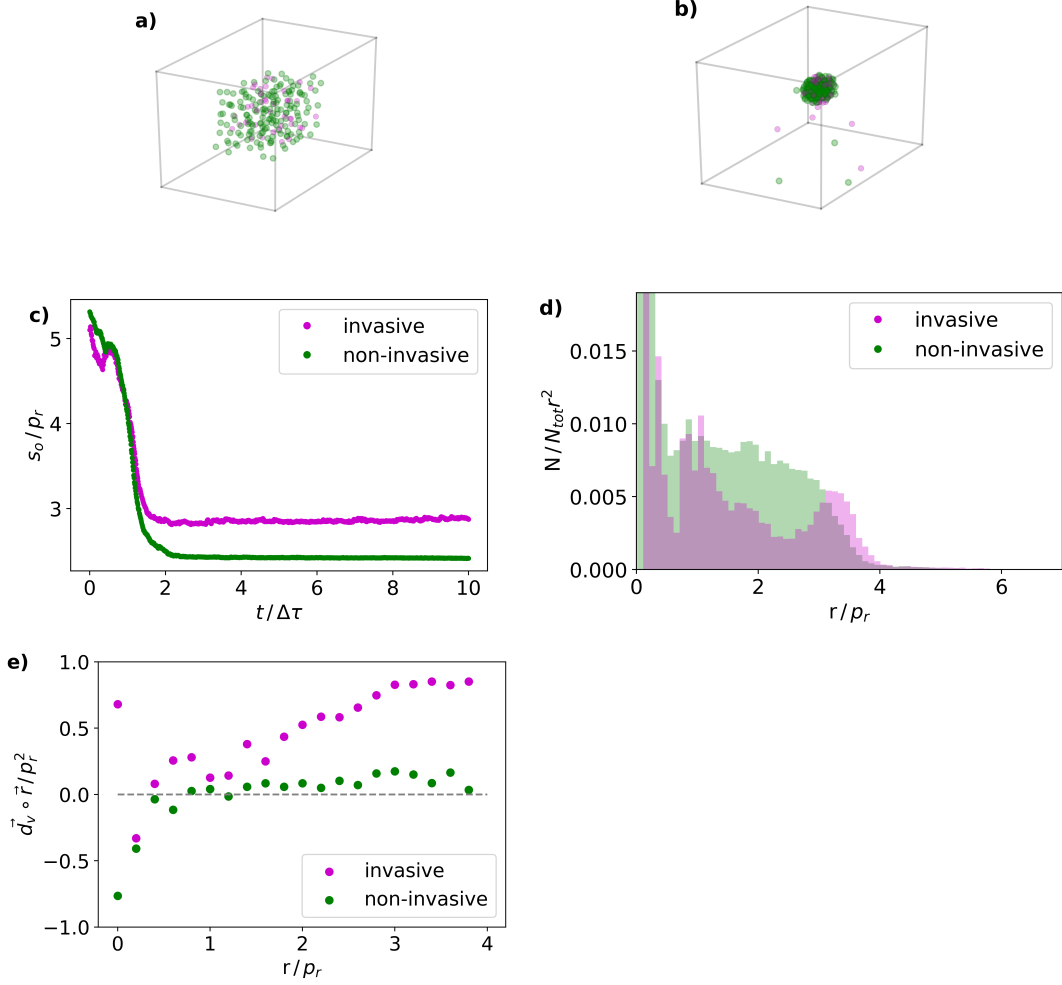


FIG. 16: Random initial conditions. The cells differ only by the strength of the activity. 10 simulations are averaged. **a:** Example of one representative initial state. **b:** One representative final state. **c:** The development of the system averaged over all 10 simulations. The invasive cells have due to their bigger activity a slightly higher probability to be on the surface of the ball. **d:** A histogram of the distances of the particle types to the center of mass, normed on the particle number, scaled with $\frac{1}{r^2}$, averaged over simulations and time. Not much difference between invasive and non-invasive cells can be seen. **e:** The alignment of the directions of the particles with respect to the center of mass, averaged over the simulations and normalized on the particle number. We see that there is a correlation of the direction and the distance to the center for the invasive particles.

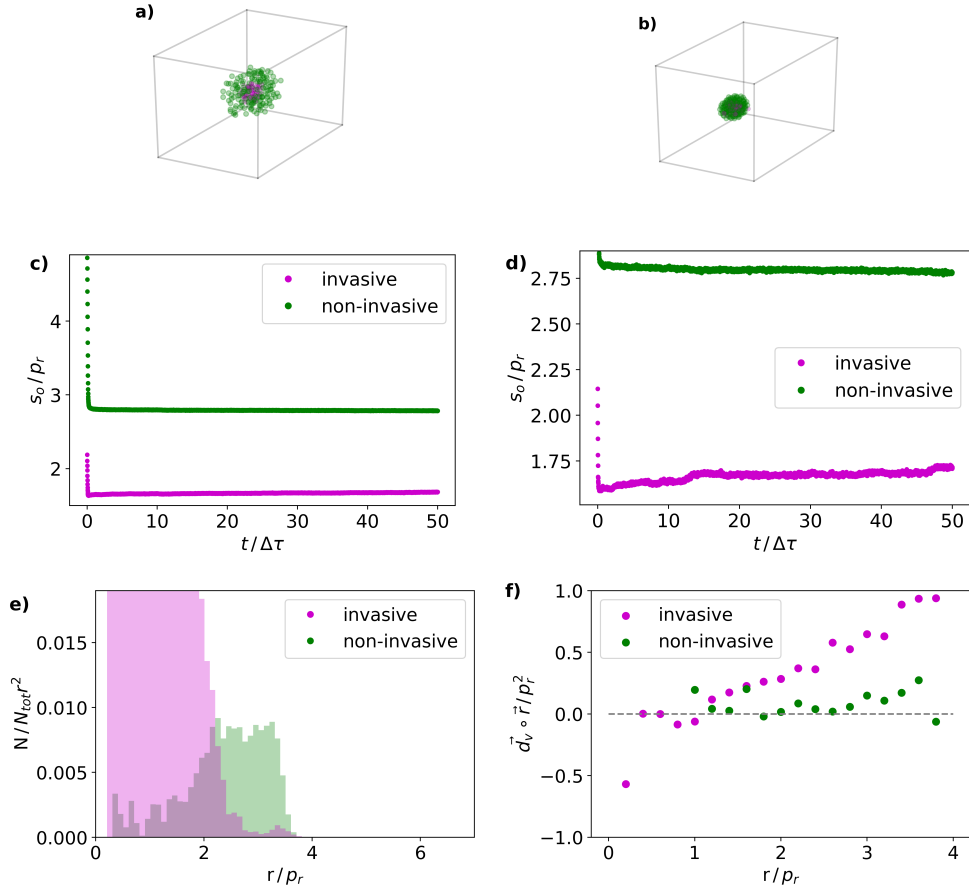


FIG. 17: Biased initial condition. The invasive cells are set in a range from $0 p_r$ to $3 p_r$ to the center, the non-invasive ones afterward from $0 p_r$ to $7 p_r$. 10 simulations are averaged. The cells differ only by the strength of their activity. **a:** Example of one representative initial condition. **b:** One representative final state. **c:** The development of the system averaged over all 10 simulations. The system seems to be stable. **d:** The development of the system for one special simulation. The steps at time $12 \Delta\tau$ and $48 \Delta\tau$ come from single particles that diffuse to the surface. **e:** A histogram of the distances of the particle types to the center of mass, normed on the particle number, scaled with $\frac{1}{r^2}$, averaged over simulations and time. One can see that there exist single invasive particles that diffuse to the surface of the ball while most of them are trapped inside. **f:** The alignment of the directions of the particles with respect to the center of mass, averaged over the simulations and normalized on the particle number. Near to the center are no non-invasive particles. Therefore there no average value could be calculated. The points where no value could be calculated are canceled.

In Figure 17 the particles are placed in a biased way. The invasive particles are placed inside the ball, while the non-invasive ones start closer to the surface. Surprisingly this configuration is stable over a long time. Only single invasive particles are able to diffuse to the surface of the ball. The main part of them is trapped inside. This is a effect that in observed in neither of the two other cases. In contrast to the case with random initial conditions, there seems to be an alignment for the non-invasive particles at the boundary of the ball. To escape to the surface a invasive particle needs their direction of activity pointing towards the surface, hence there is a very strong correlation of nearly 1.

In Figure 18 the particles are initially placed in a biased way. The non-invasive particles are placed inside the ball, while the invasive ones are on the surface. As expected this is a relatively stable configuration. As in the case of the different stiffness the main part of the invasive particles remains close to the surface of the ball. But surprisingly there is a non-zero probability that an invasive particle diffuses to the center of the ball. The direction of activity of the invasive particles is again pointing towards the surface for the outer particles. The particles that diffuse in the ball seem to have their direction of activity pointing to the center of the ball.

A system of particle types with equal potential but different size of the activity is quite different to the ones analyzed before. The system seem to be much more stable, independently of the initial condition. Therefore the initial condition seems to be more important for the development of the system than for the two other cases.

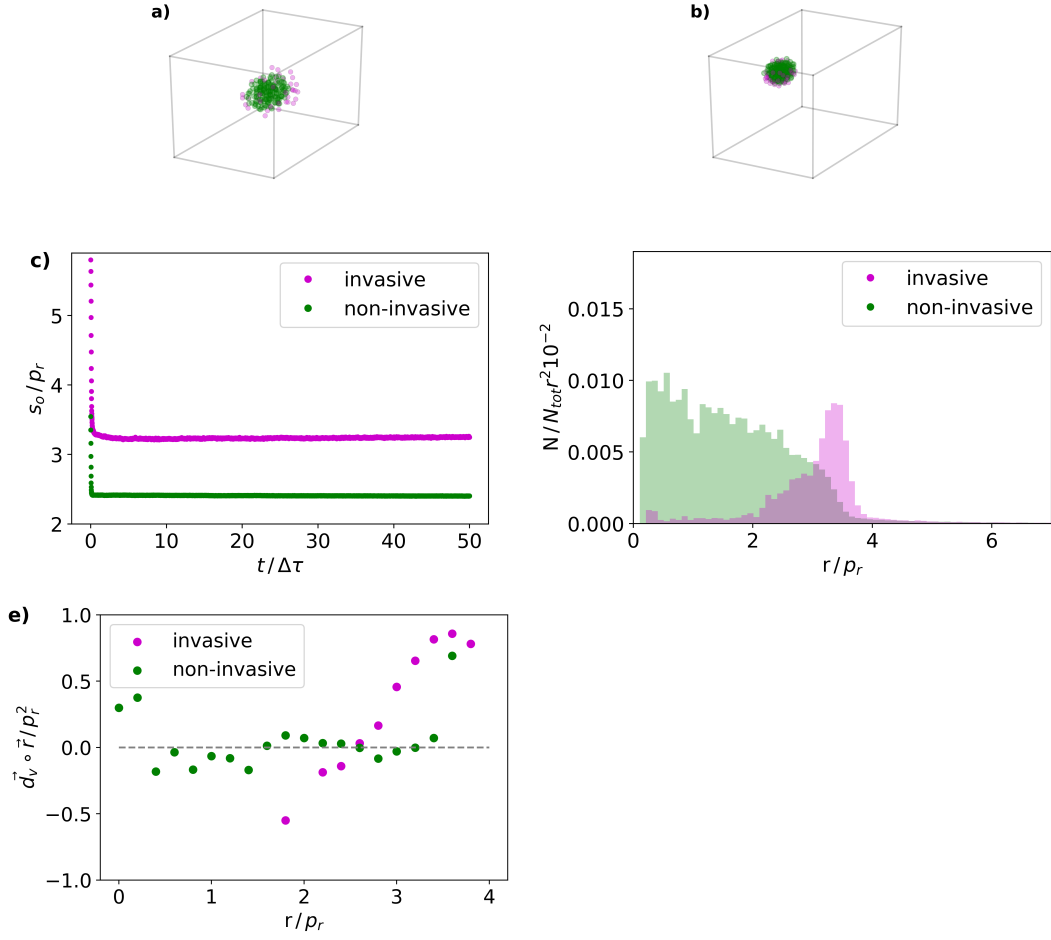


FIG. 18: Biased initial conditions. The non-invasive cells are set in a range from $0 p_r$ to $5 p_r$ to the center, the invasive ones from $5 p_r$ to $7 p_r$. 10 simulations are averaged. The cells differ only by the strength of their activity. **a:** Example of one representative initial condition. **b:** One representative final state. **c:** The development of the system averaged over all 10 simulations. In the beginning there is a relaxation to a dense ball of cells, afterward the system remain stable. **d:** A histogram of the distances of the particle types to the center of mass, normed on the particle number, scaled with $\frac{1}{r^2}$, averaged over simulations and time. **e:** The alignment of the directions of the particles with respect to the center of mass, averaged over the simulations and normalized on the particle number. Near to the center are no invasive particles. Therefore there no average value could be calculated. The points where no value could be calculated are canceled.

6. SUMMARY AND OUTLOOK

The goal of this work was to characterize which effects could lead to demixing processes between two types of particles that can be seen in experiments like Figure 1. More precisely the question was asked if the demixing can occur due to different sizes of the particles, due to a different stiffness of the particles or due to different activity. In all 3 cases it was observed that one particle type has a preference to be on the surface of the particle ball, which fits the experimentally observed behavior. We also found that some cases dependent stronger on the initial conditions (active particles) than others (particles with different size).

The other two effects seen in that experiment, the clustering of the particles and the building of a hole inside the ball have not been observed yet in simulations. Most likely the potentials of the particles could be tuned such that a clustering of particle types occur. Maybe one needs to simulate larger particle numbers to see clustering effects. The disadvantage is that the simulation time increases with N^2 in the current implementation and also it seemed that ordering processes take longer times with larger particle numbers. Therefore, this kind of simulation was not manageable here.

The second effect, the creation of the hole, can maybe be caused by the activity of the particles. In the case that the particle activity directions would align in such a way that they can collectively overcome the surface tension produced by the pair potentials, such an effect in principle is possible. Most likely this would need the fine tuning to the point where the activity is just not large enough to overcome the surface tension as a single particle.

Therefore, the behavior that is observed in the experiment is most likely a result of a mixture of the discussed effects, meaning one could possibly reproduce it with a simulation where the particle types not only differ by the interaction potential, but also by the strength of their activity. This could be the topic of ongoing research in the future.

-
- [1] M.Cóndor, C.Mark, R.C.Gerum, N.C.Grummel, A.Bauer, J.M.Gracia-Aznar, and B.Fabry. Breast cancer cells adapt contractile forces to overcome steric hindrance. *Biophysical Journal*, 116:1305–1312, 2019.
- [2] T.J.Grundy, E.D.Leon, K.R.Griffin, B.W.Stinger, B.W.Day, B.Fabry, J.C.Whit, and G.M.O’Neill. Differential response of patientderived primary glioblastoma cells to environmental stiffness. *Scientific Reports*, 6:23353, 2015.
- [3] J.R.Siewert, M.Rothmund, and V.Schumpelick. Praxis der Viseralchirurgie. *H.Vogelsang*, 2006.
- [4] N. Markwardt. Optische Tumor- und Blutgefäßdetektion zur Erhöhung von Präzision und Sicherheit bei der Stereotaktischen Biopsie von Hirntumoren. *Dissertation*, 2018.
- [5] G.J.Lauth and J.Kowalczyk. Thermodynamik, Eine Einführung. *Springer-Verlag*, 2015.
- [6] M. Schmiedeberg. Numerical condensed matter physics. *Lecture notes*, 2013.
- [7] W.T. Cofey and Y.P. Kalmykov. The langevin equation. *World Scientific*, 2017.
- [8] Cory Simon. Generating uniformly distributed numbers on a sphere. [Online; on 08.01.2020, 15:24 Uhr].
- [9] T. M. Koch. 3d traction forces in cancer cell invasion. *Dissertation*, 2012.

7. EIDESSTATTLICHE ERKÄRUNG

Hiermit versichere ich, dass ich die vorliegende Arbeit selbstständig verfasst und keine anderen als die angegebenen Quellen und Hilfsmittel benutzt habe, dass alle Seiten der Arbeit, die wörtlich oder sinngemäß aus anderen Quellen übernommen wurde, als solche kenntlich gemacht sind und dass die Arbeit in gleicher oder ähnlicher Form noch keiner Prüfungsbehörde vorgelegt wurde.

Erlangen, den 27. Januar 2020

Martin Majewski